

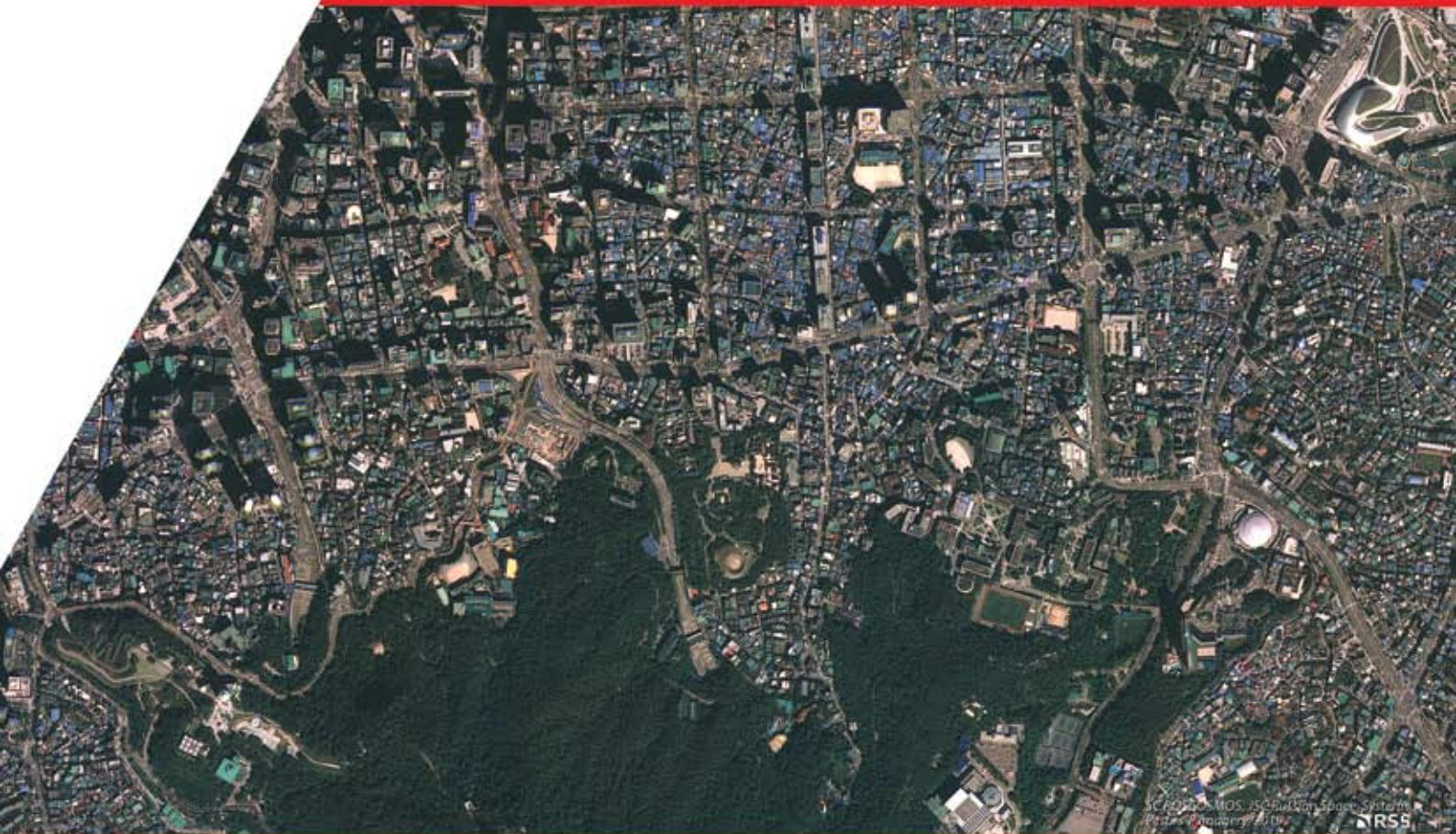


FROM IMAGERY TO DIGITAL REALITY:

Earth Remote Sensing & Photogrammetry

19th International Scientific and Technical Conference

Conference Proceedings



Organizers



Racurs
(Russia)



SI Imaging Services
(Republic of Korea)

Sponsors



ROSCOSMOS

Platinum Sponsor




Roscartography

Gold Sponsor

**MAXAR
AIRBUS**

Silver Sponsors



Resurs-P

High resolution optical-electronic sensor

Panchromatic mode / Multispectral mode (1 / 3.4 m)

High resolution sensor (SHMSA-VR)

Panchromatic mode / Multispectral mode (12 / 23.8 m)

Medium resolution sensor (SHMSA-SR)

Panchromatic mode / Multispectral mode (60 / 120 m)

Hyperspectral sensor (GSA)

96 spectral bands (30 m)



Brussels Airport, Belgium, Resurs-P satellite image

© All rights reserved, ROSCOSMOS, 2016

Dear colleagues!

The 19th International Scientific and Technical Conference “From imagery to digital reality: ERS & Photogrammetry” will be held in October 28 to 31, 2019, in Seoul, the Republic of Korea.

Determining the venue for the annual Racurs conference is not an easy task. The choice of one country over another is based on the vision of the market, partners’ activity, users’ interest, and our curiosity. Our decision to move to the East, to the Republic of Korea, was easier than ever. Korea is a unique country in relation to Russia. Despite the close location, this country is still very mysterious in terms of culture and technology.



The culture of “pali-pali” (faster-faster) allowed South Korea to become a world technological leader in a short time. As a result, one of the world’s best cadastre and cartography application systems was created. In just twenty years, South Korea has changed paper maps to digital ones, weekly updating data about road infrastructure and construction. This is one of the few countries that has full-fledged remote-sensing technologies, consisting of optical, radar, and UAV systems. It is no coincidence that the importance of geospatial information is emphasized by the mayor’s office of Seoul, the capital of the Republic of Korea, which rightfully occupies the sixth place in the ranking of Smart Cities of the World.

Racurs has been successfully cooperating with key Korean companies in the remote sensing and photogrammetric market, being a partner of SI Imaging Services, the exclusive distributor of KOMPSAT data. Our companies jointly export geospatial solutions based on Korean space images and Russian PHOTOMOD photogrammetric technologies. SI Imaging Services is a coorganizer of the conference.

19th International Scientific and Technical Conference
“FROM IMAGERY TO DIGITAL REALITY: ERS & Photogrammetry”
October 28-31, 2019, Seoul, Republic of Korea.



2019

CONTENT

<u>M.A. Altyntsey, M.A. Altyntseva. Forest space image decoding using the structural-statistical approach.....</u>	3
<u>F. Rodriguez. OneAtlas Platform, connect images from space to decisions on Earth.....</u>	15
<u>Alyabyev A.A., Alyabyeva A.D., etc. A single stereophotogrammetric terrain model for the tasks of territorial management in cities.....</u>	16
<u>P.S. Titarov. Identification of aerial or satellite imagery raster channels.....</u>	17
<u>P. Anashkin. From PhaseOne's aerial imagery to TrueOrtho and 3D.....</u>	24
<u>D. Kochergin. PHOTOMOD 6.5. Productivity and new functions.....</u>	29
<u>M. Petukhov. Improved productivity of 3D city mapping with a new hybrid sensor Leica CityMapper-2.....</u>	30
<u>A.S. Kirichenko, A G. Demidenko, A.E. Kruzhkov Automated Generalization.....</u>	31

Forest Space Image Decoding Using the Structural-Statistical Approach

M.A. Altyntsey, M.A. Altyntseva

Siberian State University of Geosystems and Technologies, Novosibirsk, Russia

For a long time remote sensing data (RSD) of the Earth are actively applied in various scientific goals, general duties and daily living. Every year the number of RSD users increases significantly that is connected with both increasing the number of space surveying systems and improvement of the modern computer equipment productivity. This computer equipment is capable to process a large data volume with the highest speed and degree of automation. The applications of RSD are extremely extensive. This can be creation and updating of topographic plans, search for mineral deposits, land monitoring, the prediction of negative environmental events, the determination of forest species composition. Depending on the application and the specific task space images of a certain resolution are chosen [1].

Among the majority of all tasks solved with space images the most difficult one is the recognition of forest characteristics. It is its forest species composition in particular. This task like many others is solved with various algorithms of pattern recognition theory. Each of the developed algorithms is usually able to reliably determine from space images only a certain range of natural and human-made objects. It is connected with the fact that their spectral brightness is stored in the form of pixels representing the values of the two-dimensional array in each band of a multispectral space image.

Algorithms of the pattern recognition theory make it possible to carry out decoding of space images on the basis of a predetermined link between spectral brightness values of objects and image elements. But the spectral brightness of image elements depends significantly on the type and resolution of the space surveying system, the state of the atmosphere and other factors. Therefore, it is not enough to use only spectral brightness values to decode images. It is necessary to use such an approach that would allow uniquely determining links when changing spectral brightness of pixels. Such an approach can be a joint analysis of a neighboring pixel group forming a feature vector that has to uniquely recognize an object. This approach is called the structural one [1].

As part of the structural approach when forming a feature vector a model that can uniquely identify an object is selected. These models may include various statistical models such as the minimum distance, the maximum likelihood, the Mahalanobis distance, etc. Most often the normal distribution law is applied in such models. Statistical models that correspond to a normal distribution law are called parametrical [2].

In case the distribution differs from normal one non-parametric models that are based on qualitative features should be used.

The non-parametric approach was proposed in [3, 4] according to which reference features are created at the beginning for all object classes in the form of functions of the probability density function. In [5] it was further proposed to create reference features as cumulative distribution functions. Large samples should be used when creating reference features and measurements should be made for images of reference objects.

Reference probability density functions and cumulative distribution functions for different space systems differ. Therefore it is necessary to create for each surveying system the database of functions for all object classes. Reference sites are usually selected in space images using a map for which probability density functions and cumulative distribution ones are created. Then, the functions for each decoded site are also created by applying the segmentation method to decode any other image site.

To compare the created functions with the reference ones the decision rule is chosen firstly. According to [3, 4] a Pearson correlation coefficient value is applied when comparing probability density functions. In case of comparing cumulative distribution functions the method proposed in [5] is used. The essence of the method is to calculate the minimum distance between the cumulative distribution functions representing the training sample and the tested one. The tested object will belong to that reference class if the distance from the cumulative distribution function created for that object to the cumulative distribution one created for one of the reference samples is less than for other reference ones.

Reference samples can be derived from a thematic map. The sites corresponding to a certain class of area objects are chosen. Each reference probability density function and cumulative distribution one can be constructed on the basis of one reference site or several. The number of measurements from non-parametric estimation theory must be greater than 100 [6, 7]. When selecting reference sites in a space image, the size of each site is clearly greater than that value. Each measurement is a single pixel of a space image. One of the goals of the article is to determine experimentally how many measurements should exist when creating reference functions.

A four-channel Ikonos space image for the area of Karakan forest near Berdsk city was selected as the study object. The resolution of each spectral imaging band is 3.2 m. A thematic map of the forest species composition was linked to the space image. The thematic map allowed choosing reference samples in the space image. Reference areas were chosen with the largest area for the following classes of objects: pine forest, birch forest, aspen forest, water, ground. Generation of reference functions was performed only for one reference site at the beginning. In Figure 1 the chosen reference samples of various types are shown and in Table 1 – their sizes in pixels.

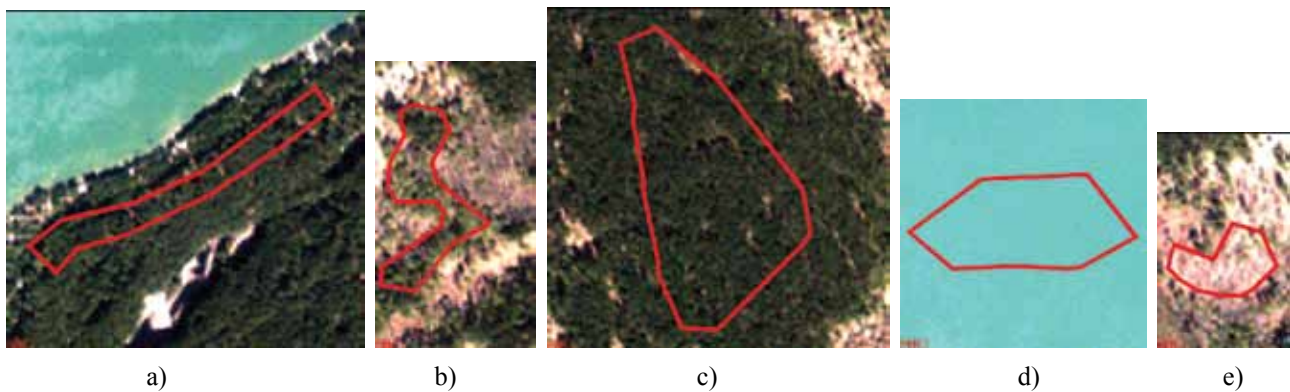


Fig. 1. Reference samples:
a) birch; b) aspen; c) pine; d) water; e) ground

Table 1. Reference site sizes

The type of a site	Birch	Aspen	Pine	Water	Ground
Pixel size	1536	1363	5748	2625	791

In order to estimate reliability of space image decoding on the basis of the given functions, tested sites were also selected from the thematic map. There were selected next test sites: 8 – pine forest, 9 – birch one, 9 – aspen one, 9 – water sites and 5 – ground. Probability density and cumulative distribution functions were constructed for each band of Ikonos image. In Figure 2 an example of constructing the probability density functions in infrared band for the reference samples and for a test sample – a part of pine forest. The largest correlation coefficient was obtained between the function of this sample and the reference function for pine forest.

In Figure 3 the example of generating cumulative distribution functions for the reference samples and the same test sample in all spectral bands.

According to Figure 3 the smallest distance was obtained between the cumulative distribution function of the test sample and this function of the reference sample for pine forest in all spectral bands.

In Table 2 the results of decoding are given. It is shown how many tested samples were correctly determined based on comparison using 2 types of functions. When comparing cumulative distribution functions there was additionally carried out the calculation of total distance over all image band that is in four-dimensional space. Additionally the birch and aspen forest were unified into a single class – deciduous forest.

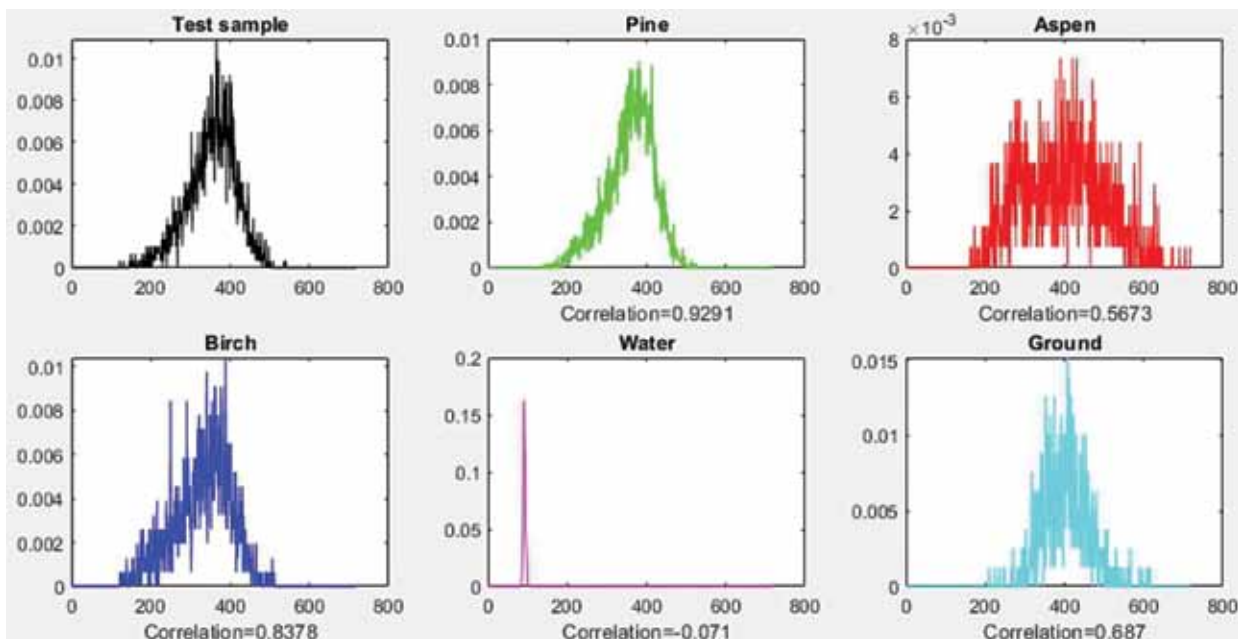


Fig. 2. The example of generating probability density functions in an infrared band

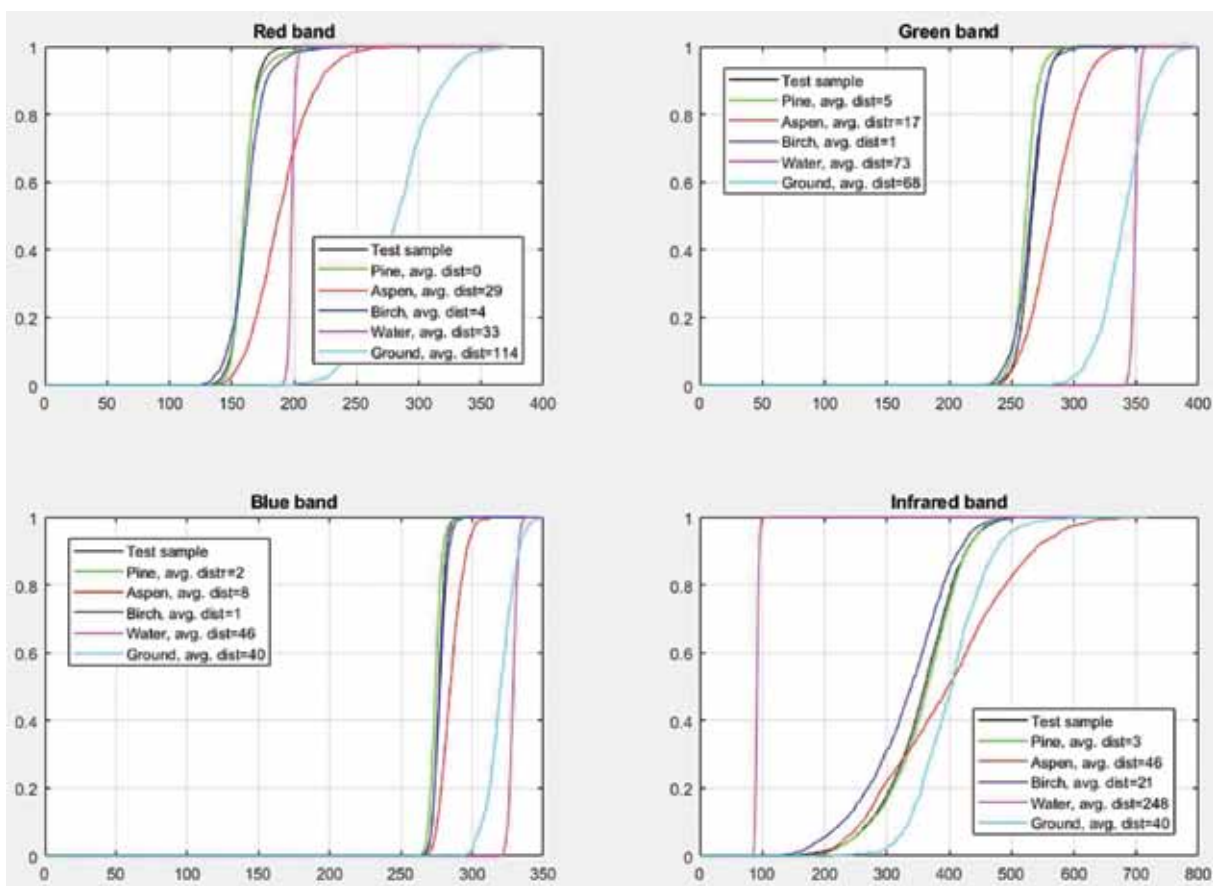


Fig.3. The example of generating cumulative distribution functions

Table 2. Results of decoding

Test sample	Band	Number of matches by cumulative distribution function	Number of matches by cumulative distribution function in 4D	Number of matches by probability distribution function
Pine	Red	8 from 8	8 from 8	8 from 8
	Blue	8 from 8		7 from 8
	Green	8 from 8		7 from 8
	Infrared	8 from 8		8 from 8
Birch	Red	1 from 9	0 from 8	1 from 9
	Blue	1 from 9		1 from 9
	Green	1 from 9		1 from 9
	Infrared	0 from 9		0 from 9
Aspen	Red	5 from 9	8 from 9	8 from 9
	Blue	8 from 9		8 from 9
	Green	8 from 9		8 from 9
	Infrared	5 from 9		2 from 9
Water	Red	7 from 9	9 from 9	3 from 9
	Blue	3 from 9		1 from 9
	Green	3 from 9		2 from 9
	Infrared	9 from 9		9 from 9
Ground	Red	0 from 5	0 from 5	0 from 5
	Blue	0 from 5		0 from 5
	Green	0 from 5		0 from 5
	Infrared	0 from 5		0 from 5
Deciduous forest	Red	13 from 18	17 from 18	18 from 18
	Blue	18 from 18		18 from 18
	Green	18 from 18		18 from 18
	Infrared	16 from 18		12 from 18

From Table 2 it is seen that reliability of decoding depends substantially on which spectral bands were selected for the decoding and which function was used for the comparison. Birch forest sites were not correctly recognized by both comparing cumulative distribution functions and probability density ones. For this reason a common class for birch and aspen forest called deciduous forest was introduced. There was also not recognized class «ground». The highest reliability of decoding was shown with the use of cumulative distribution function comparison method in four-dimensional space – 85%. In Table 3 reliability of decoding for bands and depending on the type of function is shown.

Further new reference functions constructed with several test sites were used to decode the image using the same test samples. Several reference sites in different parts of the space image were selected for each class of objects. A common cumulative distribution function and a probability density one were constructed from several reference sites of the same class. The number of measurements in common functions exceeded the data in Table 1 by an average of 7 times. In Figure 4 and 5 the result of generating new reference functions is shown.

Table 3. Reliability of decoding for bands and the type of function

Bands	Classes for comparison	Classes: pine, birch, aspen, ground, water		Classes: pine, deciduous forest, ground, water	
		Cumulative distribution function	Probability density	Cumulative distribution function	Probability density function
Red		function	Cumulative distribution function	function	73%
Blue		function	48%	73%	65%
Green		50%	45%	73%	68%
Infrared		55%	48%	83%	73%
4D space		63%	—	85%	—

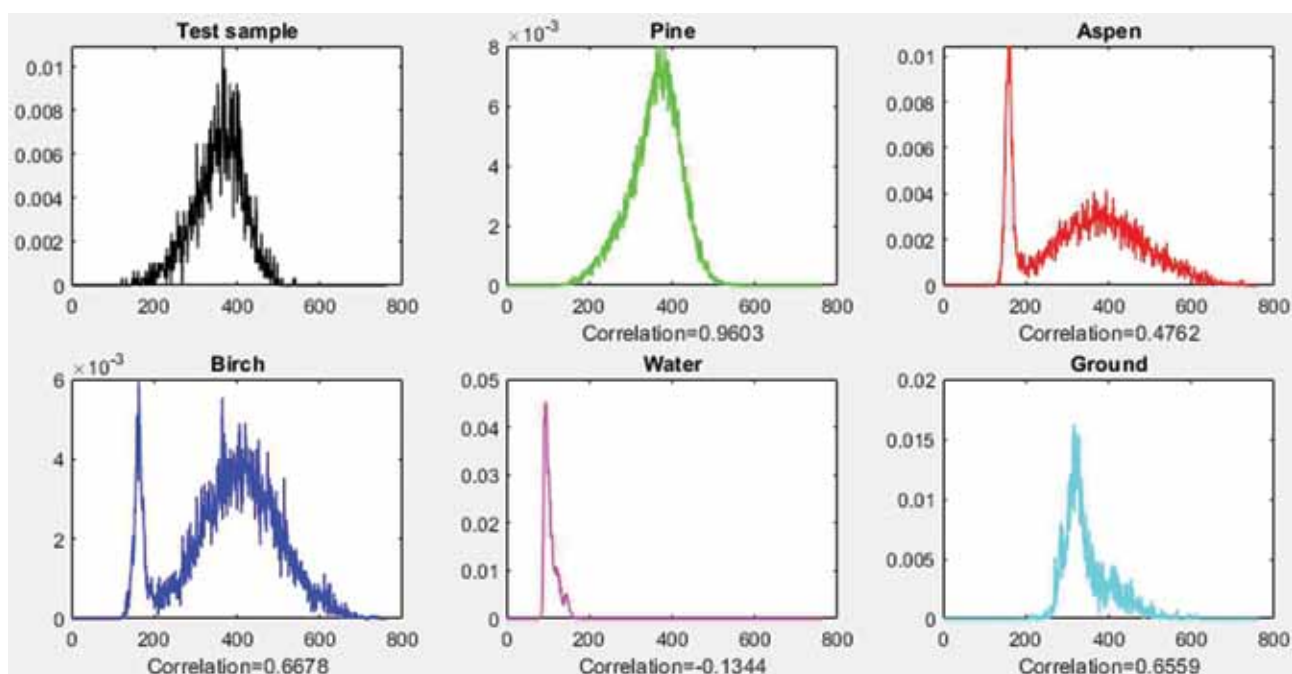


Fig.4. The example of generating new probability density functions in infrared band

The functions constructed with using a greater number of samples have more complicated form. In the example it is shown that the reference probability density functions for aspen and birch began to have 2 maximums. In Table 4 the results of decoding using these reference functions are given.

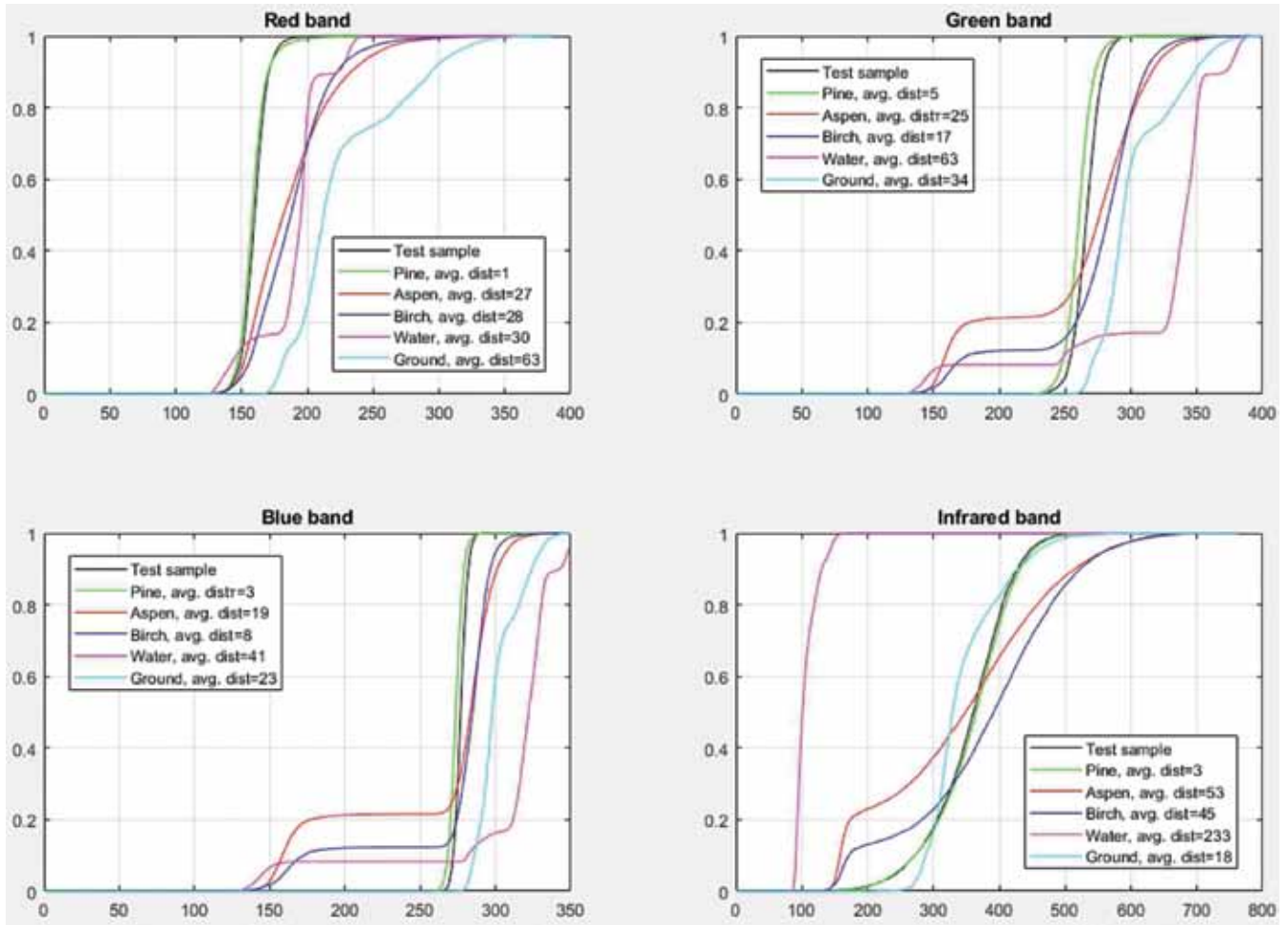


Fig.5. The example of generating common cumulative distribution functions

Table 4. Results of decoding using the common functions

Test sample	Band	Number of matches by cumulative distribution function	Number of matches by cumulative distribution function in 4D	Number of matches by probability distribution function
Pine	Red	8 from 8	8 from 8	8 from 8
	Blue	8 from 8		8 from 8
	Green	8 from 8		8 from 8
	Infrared	8 from 8		8 from 8
Birch	Red	3 from 9	7 from 9	5 from 9
	Blue	8 from 9		7 from 9
	Green	8 from 9		7 from 9
	Infrared	9 from 9		7 from 9
Aspen	Red	0 from 9	0 from 9	1 from 9
	Blue	0 from 9		2 from 9
	Green	0 from 9		1 from 9
	Infrared	0 from 9		0 from 9

Test sample	Band	Number of matches by cumulative distribution function	Number of matches by cumulative distribution function in 4D	Number of matches by probability distribution function
Water	Red	7 from 9	9 from 9	7 from 9
	Blue	7 from 9		7 from 9
	Green	7 from 9		7 from 9
	Infrared	9 from 9		9 from 9
Ground	Red	0 from 5	4 from 5	3 from 5
	Blue	0 from 5		4 from 5
	Green	0 from 5		4 from 5
	Infrared	0 from 5		5 from 5
Deciduous forest	Red	9 from 18	16 from 18	11 from 18
	Blue	16 from 18		12 from 18
	Green	15 from 18		15 from 18
	Infrared	15 from 18		11 from 18

In Table 5 reliability of decoding for bands and depending on the type of common function is shown.

Table 5. Reliability of decoding for bands and the type of common function

Bands	Classes for comparison	Classes: pine, birch, aspen, ground, water		Classes: pine, deciduous forest, ground, water	
		Cumulative distribution function	Probability density	Cumulative distribution function	Probability density
Red		function	Cumulative distribution function	function	73%
Blue		function	70%	78%	78%
Green		58%	68%	75%	85%
Infrared		62%	73%	80%	83%
4D space		70%	–	93%	–

By applying the new reference functions it became possible to correctly decode the test samples of the ground class. All samples of this class were correctly decoded using the probability density function in the infrared band as well as 4 from 5 of these samples were found with cumulative distribution function in four-dimensional space. When generating reference samples for only one site, no sample of the ground class was correctly defined. The test samples of birch and aspen forest have been identified with low reliability in both situations. And in the case when samples of this forest were combined into one class "Deciduous forest" the total decoding reliability of all samples reached 93%.

Thus, the use of reference functions created over several test sites allowed significantly increasing the reliability of space image decoding. Fragments of conifer forest and deciduous forest were reliably identified. The decision rule based on determining the minimum distance between cumulative distribution functions in a four-dimensional space demonstrated the best results of decoding. But at the same time the

recognition reliability of individual species of deciduous forest turned out to be low.

To increase the decoding reliability of individual forest species, the generation of cumulative distribution and probability density functions can be carried out using not the original bands of space images, but using transformed ones on the basis of various algorithms. More study is required both in this direction and based on the use of more test sites and space images.

REFERENCES

1. Guk A.P., Evstratova L.G., Khlebnikova E.P., Arbuzov S.A., Altyntsev M.A., Gordienko A.S, Guk A.A., Simonov D.P. Development of techniques for automated decoding of aerospace images. Object picture interpretive features on multispectral satellite images // *Geodesy and Cartography*. 2013. Vol. 7. P. 31-40.
2. Guk A.P., Evstratova L.G., Study of the efficiency criteria for estimating statistical non-parametric methods for forest decoding // *Regional Problems of Earth Remote Sensing: Proceedings of the V International Scientific Conference, September, 11-14, 2016, Krasnoyarsk: Siberian Federal University*. 2018. P. 12-15.
3. Guk A.P., Evstratova L.G. New statistical approach of forest image recognition // *Regional Problems of Earth Remote Sensing: Proceedings of the III International Scientific Conference, September, 13-16, 2016, Krasnoyarsk: Siberian Federal University*. 2016. P. 14-17.
4. Guk A.P. Automation of photo interpretation. Theoretical aspects of statistic recognition of images // *Izvestia vuzov. Geodesy and aerophotography*. 2015. Vol. 5/C. P. 166-170.
5. Guk A.P., Altyntsev M.A., Evstratova L.G., Altyntseva M.A. Algorithms of multispectral aerospace image sequential analysis based on the use of structural-statistical approach for natural object decoding // *Processing of space data in monitoring tasks of natural and human-made processes (SDM-2019): Proceedings of Russian conference (26-30 august 2019, Berdsk)*. – P. 77-83.
6. Fukunaga, K. *Introduction to statistical pattern recognition*. London: Academic Press; 2 Edition, 1990. 592 p.
7. Guk A.P., Shlyakhova M.M. Study of statistical characteristics of multispectral forest space images // *Regional Problems of Earth Remote Sensing: Proceedings of the V International Scientific Conference, September, 11-14, 2016, Krasnoyarsk: Siberian Federal University*. 2018. P. 105-108.



SMART EYES IN THE SPACE KOMPSAT SERIES

KOMPSAT-3A
40 cm

KOMPSAT-3
50 cm

KOMPSAT-2
1 m

KOMPSAT-7
30 cm

CAS-500
50 cm

EO

To be launched >>>

X-Band
SAR

To be launched >>>

KOMPSAT-5
85 cm

KOMPSAT-6
50 cm





A MAXAR COMPANY

Subscribe to the largest library of global imagery

An EarthWatch subscription gives you instant access to the best of DigitalGlobe satellite imagery and geospatial data. And you don't have to be an imagery expert or have in-house tools; EarthWatch is designed to make imagery accessible to anyone who needs it, whether you're concerned with a specific area or the entire globe.

DigitalGlobe.com/Racurs

Mapping the world

Stay informed with *GIM International*

GIM International, the independent and high-quality information source for the geomatics industry.

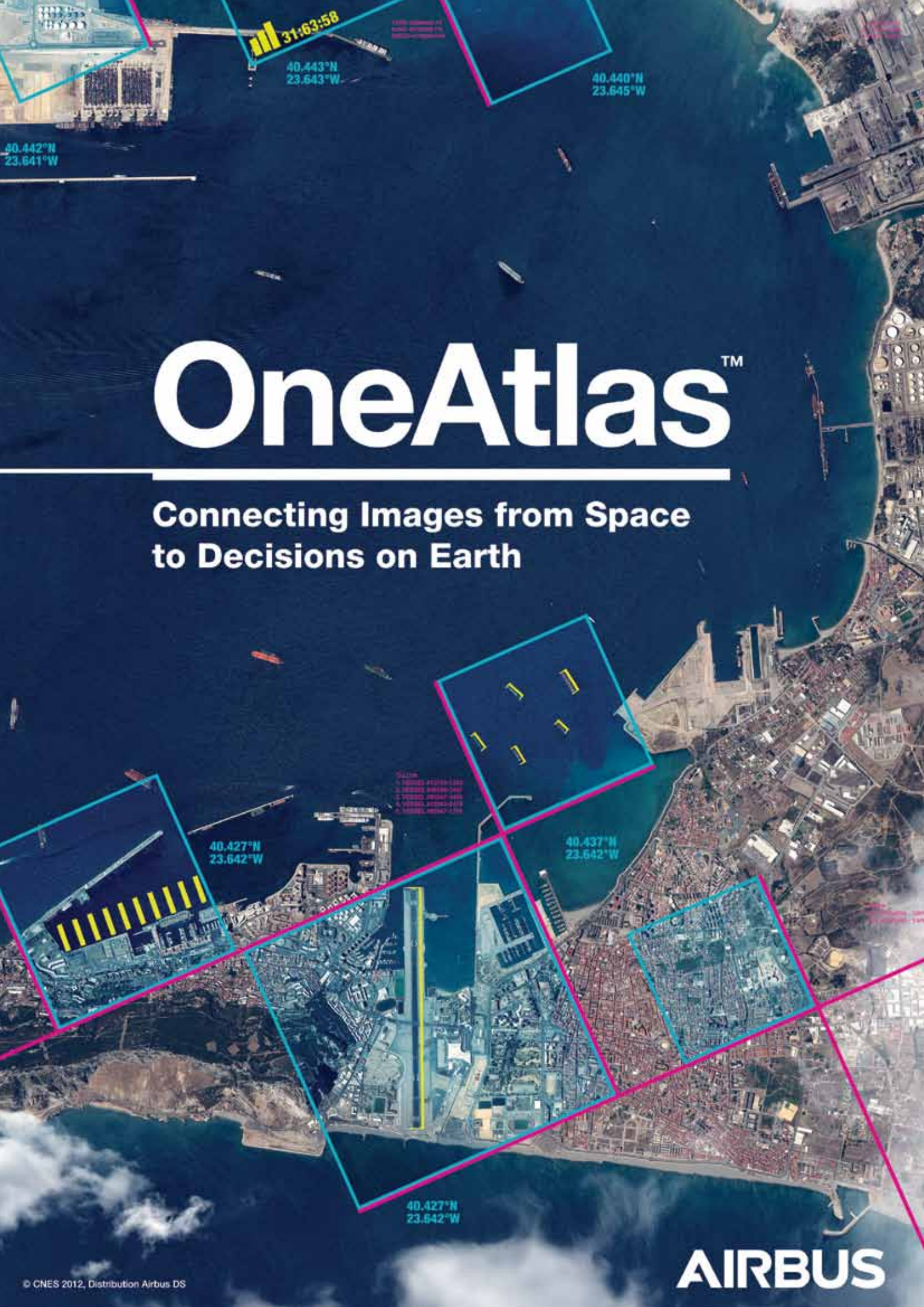
- Topical overviews
- News and developments
- Expert opinions
- Technology

Sign up for your free subscription to the online magazine and weekly newsletter today!

www.gim-international.com

GIM
INTERNATIONAL





31:63:58

40.443°N
23.643°W

40.440°N
23.645°W

40.442°N
23.641°W

OneAtlas™

Connecting Images from Space
to Decisions on Earth

Table
1. 00000 00000-000
2. 00000 00000-000
3. 00000 00000-000
4. 00000 00000-000
5. 00000 00000-000

40.427°N
23.642°W

40.437°N
23.642°W

40.427°N
23.642°W

AIRBUS

OneAtlas Platform, Connect Images from Space to Decisions on Earth

Fabrice Rodriguez, Airbus Defence and Space, France

OneAtlas provides users with premium Airbus data, thematic services and analytic capabilities that answer a variety of user and industry-specific needs. The goal of OneAtlas is to make data and services easy for users to access, to enable better informed decision-making.

Based on the Airbus constellation of satellites, partner satellites and open source data, OneAtlas Data enables imagery to be delivered in multiple and flexible ways: through streaming, download or API. Our data services include the Living Library, WorldDEM Streaming and Basemap, which provide users with access to premium Airbus imagery and fresh, global layers of information.

Our thematic services and analytic capabilities answer specific needs of our customers. From no-deforestation verification services (Starling) to turn-key analytics that provide biomass and nitrogen information (Verde) to ship detection (Ocean Finder) and monitoring oil refineries to help predict shutdowns (RefineryScanner). OneAtlas offers a variety of industry-specific services, to name a few.

With over 30 years of remote sensing expertise Airbus is a reliable and trust-worthy provider.

In today's world, information is everything, but it can be a challenge to come by the right information at the right time and in the right format. Airbus Intelligence supports its customers with technologies and capabilities to strengthen how they plan and respond to challenges and missions – with greater speed and higher certainty.

With over 30 years of experience in Earth observation, we provide sustainable solutions that deliver exactly what our customers need, when they need it, where they need it.

The OneAtlas Platform is the entry point for instant access to Premium Airbus data, Analytics and Thematic Services.

OneAtlas Data: A unique place for quick and easy access to updated imagery and layers of information.

The Living Library: offers access to premium Airbus imagery in multiple formats including streaming, download and API. Imagery within the Living Library is constantly being updated and users can stream imagery at full resolution, with no minimum order size.

Basemap: Empowers users with the most reliable context, over anywhere in the world. This global layer is made from our highest grade satellite imagery and constantly refreshed – with no pixel being older than 1 year. Basemap is 1.5m global coverage, with 50cm coverage over 2,000 urban areas, available via API or download it into your own GIS.

WorldDEM Streaming: Complete pole-to-pole coverage coupled with unrivaled accuracy and quality, WorldDEM Streaming provides global* access to WorldDEM and WorldDEM4Ortho via streaming for 3D analytics and generating value-added information. Users only pay for what they need with no minimum order size, and available in flexible packages, depending on custom needs.

*On demand release request for sensitive countries

With the newly launched OneAtlas plugin in Photomod users can access directly from their working environment to the OneAtlas content, get some intelligence, take decision and generate value added products.

**A single stereophotogrammetric terrain model
for the tasks of territorial management in cities**

*Alyabyev A.A., Alyabyeva A.D., Grachev A.V., Nikitin V.N.,
Ural-Siberian Geoinformation Company, Ekaterinburg, Russia*

The most of the current tasks of municipal administration, urban planning, land and property activities in cities and other settlements are solved on the basis of spatial information about the area with errors in determining the coordinates of points up to 10-20 cm in plan and 15-25 cm in height.

The modern development of technical and hardware-software systems allows the use of the stereophotogrammetric method to obtain spatial data about the area with the above accuracy. The use of stereo models for solving tasks in the territories of settlements makes it possible to obtain visual and metric information about the terrain on the ground as necessary.

USGIK JSC developed and registered a software product called “Informational stereoscopic image of the territory” (INSOT). The program provides: three-dimensional visualization of a seamless stereoscopic model of the territory based on aerial photographs; three-dimensional visualization of vector data and 3D-models of objects; support for polarization, line by line, shutter and anaglyphic modes of stereo imaging; taking measurements according to a stereoscopic model.

A single stereo model of the city makes it possible, on the one hand, to observe the general spatial picture of the territory, and on the other hand, to make necessary and detailed measurements of the terrain objects in detail and with high accuracy. The use of such a resource allows updating urban planning documentation, performing control and licensing functions, and obtaining information on urban infrastructure facilities regardless of the time of year. Monitoring the territory by updating the stereo model is much faster and cheaper than using maps, 3D-models and orthophotomaps.

The supply of a single stereophotogrammetric terrain model is made by USGIK JSC on the orders of municipalities in addition to the standard set of products and services based on the PHOTOMOD DPW for customers workplaces. The standard complex includes: Core and StereoDraw modules, a balanced photogrammetric design, CM1 stereo monitors of own production, user training in working with software and the skills of stereoscopic measurements of objects of interest.

Development of normative documentation in the process: draft national standard “TECHNOLOGY FOR CREATING A HIGH-PRECISION STEREO MODEL OF A LOCATION Technical requirements” is included in the national standardization plan for 2019 and is currently being prepared for submission to Rosstandart for editing.

Identification of Aerial or Satellite Imagery Raster Channels

P.S. Titarov, Racurs, Moscow, Russia

Introduction

As the experience of everyday work shows, some photogrammetry specialists, being professionally focused on the geometric aspects of image processing, may become confused if the software they use to handle multispectral aerial or satellite imagery fails to match the raster channels to the spectral bands. This problem often occurs when new imagery products are introduced into the market and the software is not completely compliant with them or some errors have not been revealed and fixed yet. It may also be caused by the absence of the image metadata. Trying all possible channels-to-bands matches would be a rather time-consuming approach.

This article does not provide an exhaustive survey of the problem; it is merely a case study, which nevertheless may be useful as far as it considers a rather common situation, so the approach described here may be of some help if the routine workflow runs into difficulties of this sort.

Problem description

This case study considers processing a four-band (blue, green, red and near infrared) multispectral satellite image which is a part of a new imagery product (which, in fact, is still under development and has not been released yet). Immediately after the image has been imported into a digital photogrammetric system (PHOTOMOD software package) the raster looks like shown in Fig. 1.



Fig. 1: The image immediately after being imported into photogrammetric software.

The default procedure applied for matching the raster channels to the spectral bands has obviously failed. PHOTOMOD software allows the user to see the numbers of the channels assigned to the red, green and blue bands (see Fig. 2):

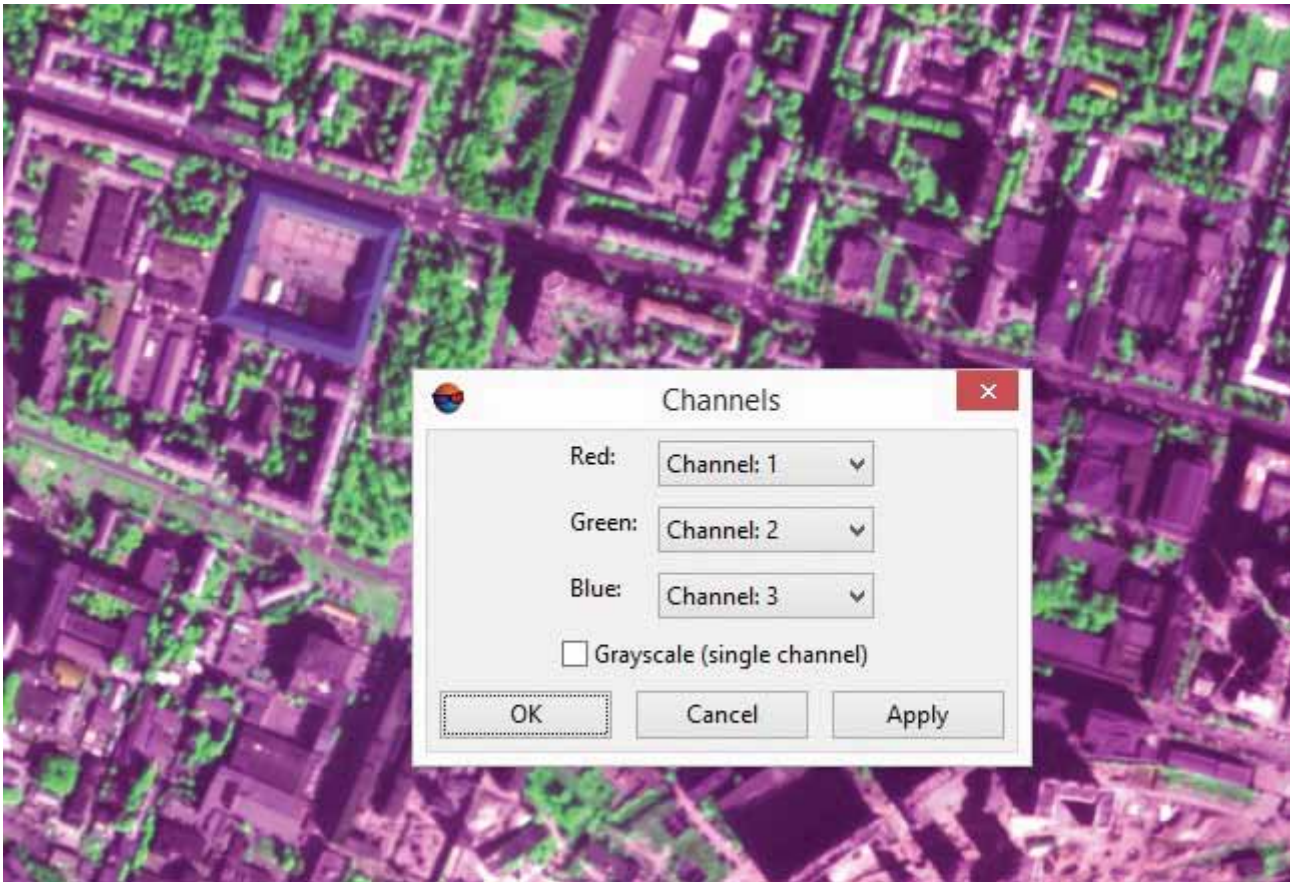


Fig. 2: The raster channels assigned to the spectral bands by default.

At first glance it may seem that the channel number for the green band is assigned correctly as far as the foliage is displayed in green; its unnatural shade may be accounted for by the channel mismatch for other bands. But let us avoid hasty judgments.

Spectral bands identification

Let us look at a fragment of the image which contains vegetation and set all the three color raster channels (red, green and blue) to display the same spectral band — for each band by turns. Fig. 3 shows it for the spectral band corresponding to raster channel 1:

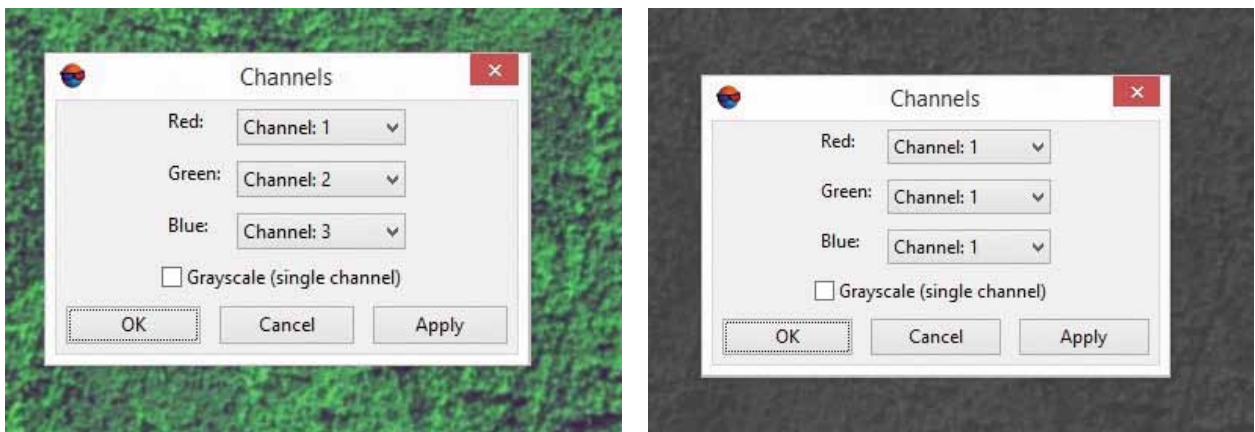


Fig. 3: Setting all three colour raster channels to display the same spectral band.

It is needless to say that the image will be looking grayscale - but not the same for different spectral bands.

Let us compare the grayscale rasters corresponding to different channels/spectral bands:

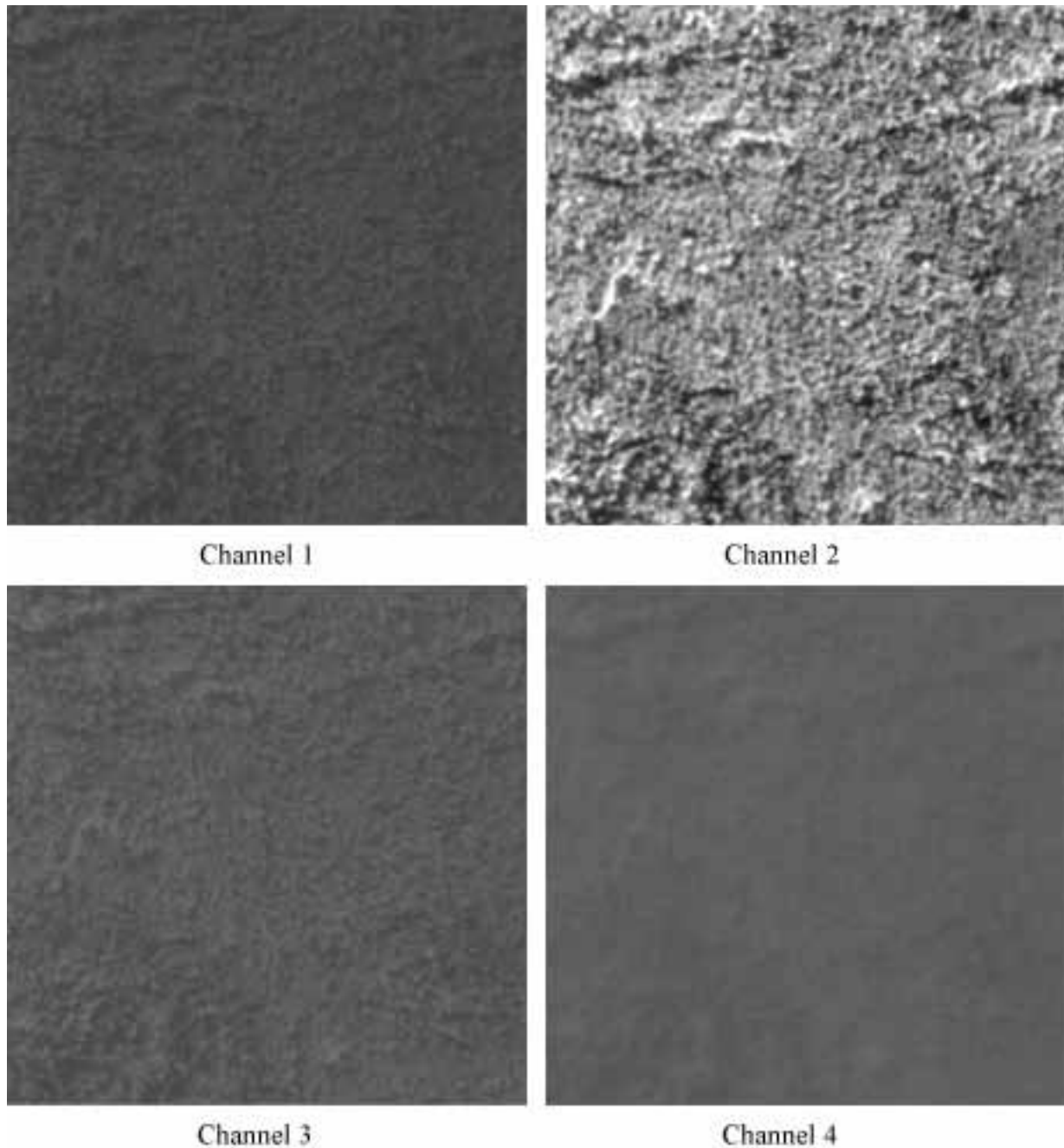


Fig. 4: Vegetation displayed in different channels.

Firstly, the raster corresponding to channel 4 evidently is the most blurred one. Under the meteorological conditions the imagery is acquired the blurring is caused by Rayleigh scattering; the shorter the wavelength the stronger is the scattering, therefore, it is the blue band which is most affected by it (it is commonly known that this type of scattering makes the clear sky blue). So channel 4 quite likely corresponds to the blue spectral band.

Secondly it leaps to the eye that vegetation looks the brightest in the raster corresponding to channel 2.

It might be assumed that vegetation which looks green to us should be the brightest in the green spectral band. But let us remember the limitations of human vision and consider the diagram describing vegetation spectral reflectance (see Fig. 5):

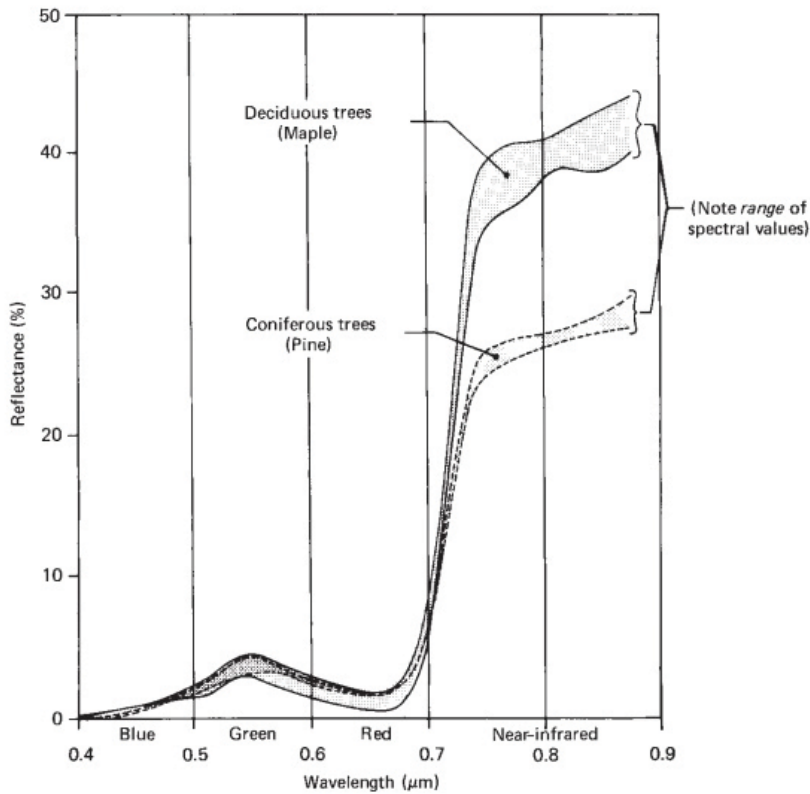


Fig. 5: Generalized spectral reflectance envelopes for deciduous (broad-leaved) and coniferous (needle-bearing) trees (adapted from [3], Fig. 1.7, page 14).

The diagram shows that vegetation reflectance in the green band is somewhat higher than in red and blue ones, but in terms of quantity the difference between all the three color bands is fairly small as compared to much higher reflectance value in the near infrared band!

On the other hand, at the surface of the Earth solar radiance in the near infrared spectral band is significantly lower than in the green one (see Fig. 6):

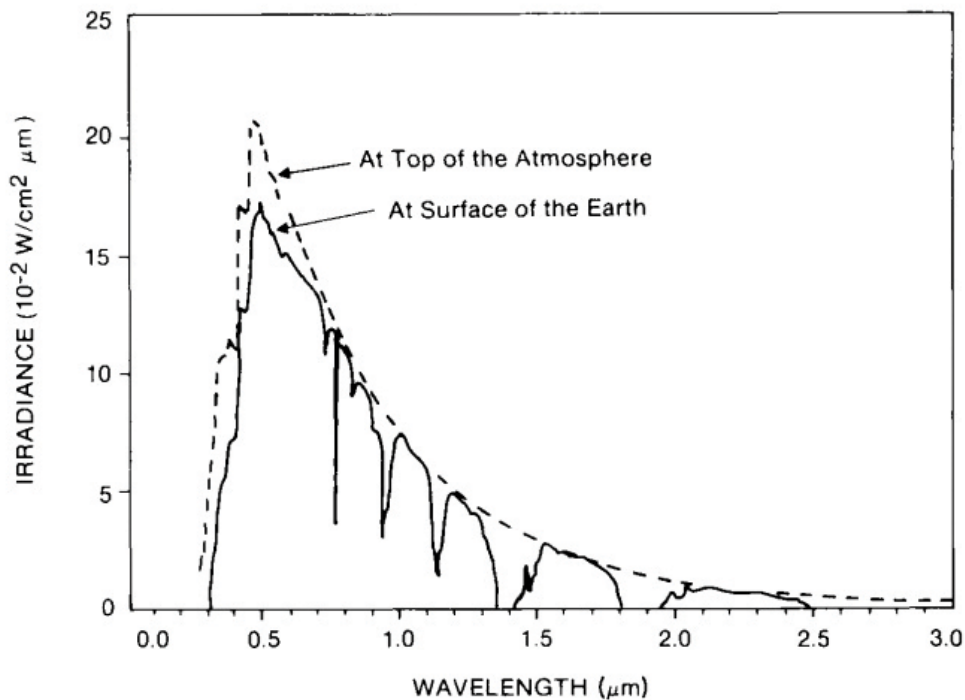


Fig. 6: Solar spectral radiance as a function of the wavelength at the top of the atmosphere and at the surface of the Earth (adapted from [2], Fig. 1.3, page 11).

Hence although there are some reasons to conclude that channel 2 corresponds to the near infrared band it would be a good idea to provide another evidence for this conclusion. For this let us find in the image some water bodies which should look dark in the near infrared band as far as the reflectance of water in this band is significantly lower than in the visible range (see the dotted line in Fig. 7):

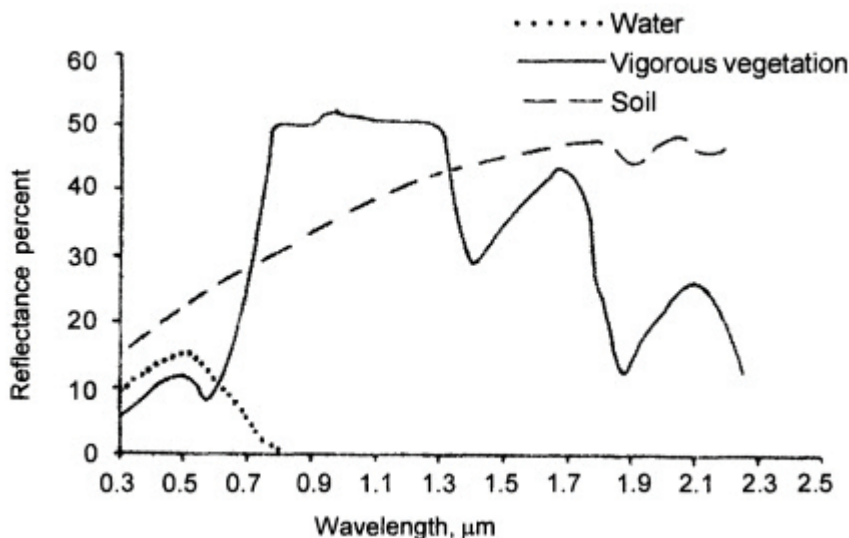


Fig. 7: Spectral reflectance curves or spectral signatures of typical features of earth's surface (adapted from [1], Fig. 2.15, page 47).

In the same way we did it before let us produce the rasters showing the water body in different channels:

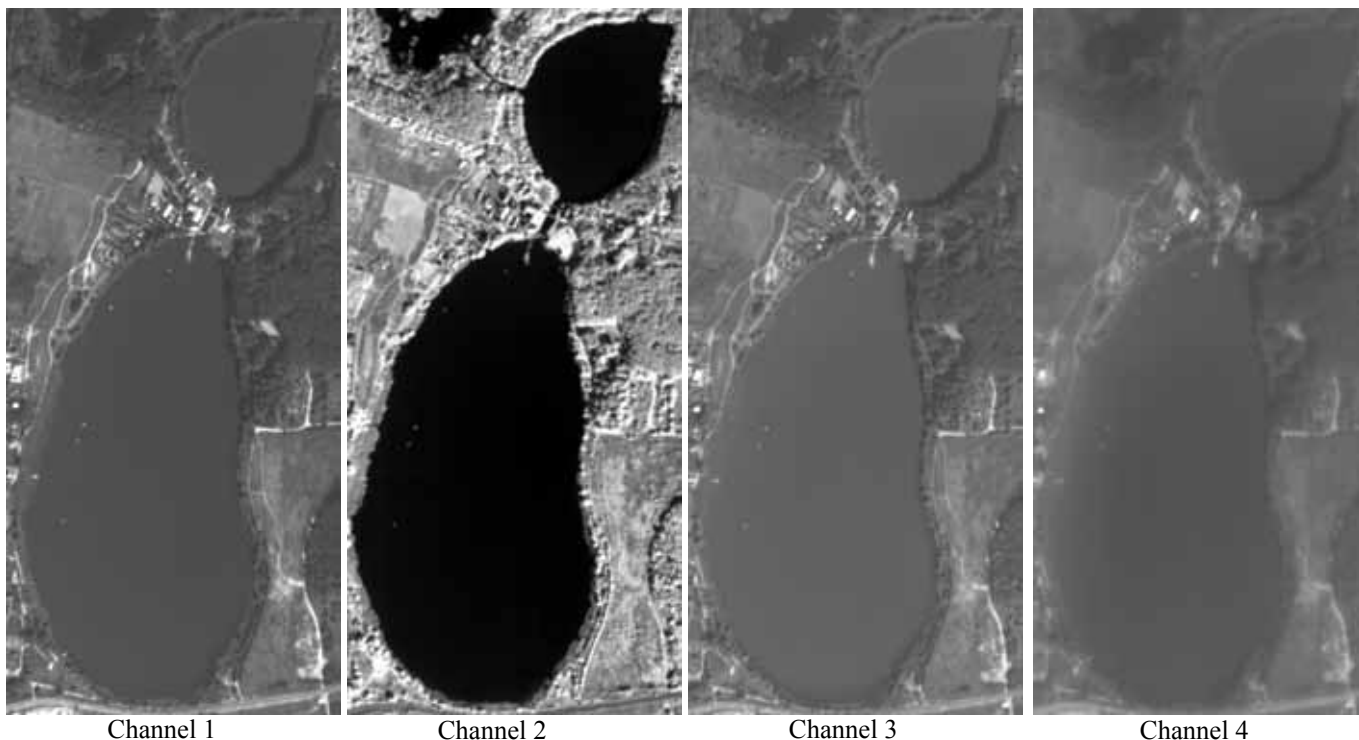


Fig. 8: A water body displayed in different channels.

In the channel 2 raster the water body looks much darker than in other channels while the brightness of the surrounding vegetation is much higher. Moreover, even in the downscaled fragments shown in Fig. 8 we can see that the image representing channel 4 (which most probably corresponds to the blue band) is the most blurred one while channel 2 image is the sharpest — this fact, taking into account the

Rayleigh scattering, also suggests that channel 2 corresponds to the longest wavelengths available in the multispectral image — in other words, to the near infrared band.

So channels 2 and 4 most probably contain the near infrared and blue band data respectively. Considering the other two channels, channel 1 and channel 3, the latter one seems to correspond to the green band as far as vegetation looks brighter in it than in channel 1 (see Fig. 4). So if channel 3 is assumed to be green, channel 1 has to be red. It should be noted that this channel numbering is neither common nor self-evident.

Verification of raster channels identification

To check the conclusions we have come to, let us set the software to display channels according to our findings: channel 1 data as red, channel 3 data as green and channel 4 data as blue. Very convenient objects for the verification are stadiums: during the imagery acquisition season the football field is usually green and the race tracks around it are red. Although sometimes the colors are different (for example, the race tracks may be black), they do not vary as widely as the color of roofs which can be gray, red, blue, green and so on.



Fig. 9: Stadiums in the raster displayed according to the found channels-to-bands matching.

In the Fig. 9 we can see that the stadiums are displayed in the right colors, vegetation is green and its shade seems to be quite natural and other objects look natural as well.

In case the image covers an undeveloped area and there are not enough human-made objects for reliable verification one can make use of Google Earth service. The author once came across an image which seemed to be looking quite unnatural but actually it was the true colors of a landscape in South America.

Besides that, most imagery products include a quicklook file which can be used to check whether the image is displayed correctly.

Fig. 10 below shows the same raster fragment as Fig. 1 to compare the correct channels-to-bands matching with the default one.



Fig. 10: The raster shown in Fig. 1 after channels-to-bands matching correction.

Conclusion

The following procedure to match the channels of a four-channel multispectral aerial or space image to the spectral bands (blue, green, red and near infrared ones) is proposed:

1. Display a fragment of the image covering vegetation in each channel separately. The channel of the most blurred raster is likely to correspond to the blue spectral band, the channel of the brightest raster most probably belongs to the near infrared band; the brighter of the other two rasters corresponds to green and the remaining one — to the red band.
2. Examining the vegetation it is possible to confuse the green band with the near infrared one, so for reliable identification of the near-infrared band it is useful to display a water body in each channel separately. It will be looking the darkest in the near-infrared band.
3. Very convenient objects for the verification of channels-to-bands matching are stadiums; besides that one can make use of Google Earth service or the quicklook included in most imagery products.

References

1. Anji Reddy M., Textbook of Remote Sensing and Geographical Information Systems, 3rd ed., Hyderabad: BS Publications, 2008.
2. Chen H.S., Space Remote Sensing Systems: An introduction.: Academic Press, 1985.
3. Lillesand T.M., Kiefer R.W., Chipman J.W., Remote Sensing and Image Interpretation, 7th ed.: Wiley, 2015.

From PhaseOne's Aerial Imagery to TrueOrtho and 3D

P. Anashkin, JSC Uralgeoinform, Yekaterinburg, Russia

For 2018 and 2019 JSC Uralgeoinform carried out aerial photography of the territories of several regions of the Russian Federation, such as the Republic of Bashkortostan, the Republic of Tatarstan, Novosibirsk region, Samara region. Aerial photography was carried out using the Phase One 190MP Aerial System. Based on the aerial photography, the following products were created:

- Ortho, navigation maps of scale 1:2000 for cities with a population of more than 1 million people, such as Novosibirsk, Volgograd, Samara, Ufa;
- Ortho at the scale of 1:10000 for other settlements and inter-settlement territories.

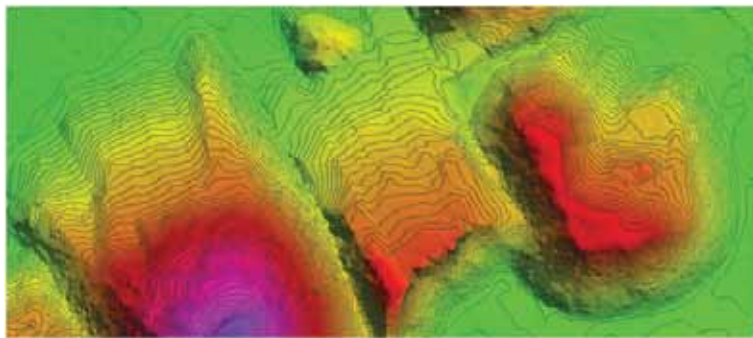
The report presents the results of photogrammetric processing of big data obtained from aerial photography via the PHOTOMOD.

Methods of processing photogrammetric projects both in automatic mode and with the use of manual correction in the PHOTOMOD to create dense point clouds are presented.



In the process of automatic processing of dense point clouds, digital terrain models and digital terrain models were built. Subsequent verification and analysis of the obtained digital terrain models

showed their high degree of detail and metric accuracy, satisfying the acceptable average errors of the terrain topography for this type of terrain.



The report describes the work on creating TrueOrtho in PHOTOMOD 6.4 based on several images of spatial objects taken at different angles with significant longitudinal and transverse overlap.

settings are proposed for obtaining high-quality textured 3D terrain models.

Satisfactory compatibility of 3D models created in the PHOTOMOD with computer-aided design systems of well-known manufacturers has been proven.

Options for optimal the PHOTOMOD software

GeoConnexion



FROM LOCAL TO GLOBAL:
THE LATEST NEWS, STORIES AND REPORTS
FROM GEOTECHNOLOGY INDUSTRIES AROUND THE GLOBE
AVAILABLE IN PRINT, ONLINE & ON DIGITAL

FREE SIGN UP NOW

GEOSPATIAL DATA, BIM, SMART CITIES, GNSS, GIS, SATELLITE IMAGERY, UAS, GPS, SURVEYING, VISUALISATION OF 3D GEODATA, AIRBORNE LIDAR, INDOOR MAPPING, MOBILE MAPPING, PHOTOGRAMMETRY & POINT CLOUDS **AND MORE ...**

GEOCONNEXION.COM

GEO Informatics

Knowledge for Surveying, Mapping & GIS



Geo-IT Professionals depend on GeoInformatics as an information source helping them to do their jobs better. Through our website, newsletters and Social Media Channels we serve more than 30.000 dedicated Geo-IT Professionals world-wide!

GeoInformatics aim is to be an independent easily accessible information source providing up-to-date news for all Geospatial Professionals, world-wide!

Be part of GeoInformatics and subscribe for free to our newsletter at www.geoinformatics.com

www.geoinformatics.com



an Open Access Journal by MDPI



Editor-in-Chief

Dr. Prasad S. Thenkabil

Section Editor-in-Chief

Prof. Dr. Clement Atzberger Dr.

Richard Gloaguen

Prof. Dr. Alfredo R. Huete

Dr. Xiaofeng Li

Dr. Richard Müller

Prof. Dr. Randolph H. Wynne

Dr. Qi Wang

Prof. Dr. Soe Myint

Dr. Magaly Koch

Prof. Stuart Phinn

Dr. Vincenzo Levizzani









Remote Sensing
Editorial Office
remotesensing@mdpi.com

MDPI, St. Alban-Anlage 66
4052 Basel, Switzerland
Tel: +41 61 683 77 34
Fax: +41 61 302 89 18

Message from the Editorial Board

Remote Sensing is now a prominent international journal of repute in the world of remote sensing and spatial sciences, as a pioneer and pathfinder in open access format. It has highly accomplished global remote sensing scientists on the editorial board and a dedicated team of associate editors. The journal emphasizes quality and novelty and has a rigorous peer-review process. It is now one of the top remote sensing journals with a significant Impact Factor, and a goal to become the best journal in remote sensing in the coming years. I strongly recommend Remote Sensing for your best research publications for a fast dissemination of your research.

Author Benefits

-  **Open Access** Unlimited and free access for readers
-  **No Copyright Constraints** Retain copyright of your work and free use of your article
-  **Impact Factor 4.118** (2019 Journal Citation Reports®)
-  **Thorough Peer-Review**
-  **Coverage by Leading Indexing Services** SCIE-Science Citation Index Expanded (Clarivate Analytics), Compendex(Ei) / Engineering Village (Elsevier), Scopus (Elsevier)
-  **Remote Sensing Ranked** No.1 Open Access Journal and 7th among All Journals in the Remote Sensing Subject Category
-  **No Space Constraints, No Extra Space or Color Charges** No restriction on the length of the papers, number of figures or colors
-  **Discounts on Article Processing Charges (APC)** if you belong to an institute that participates with the MDPI membership program

Improved Productivity of 3D City Mapping With a New Hybrid Sensor Leica CityMapper-2

M. Petukhov, Hexagon Russia, Moscow, Russia

The need for accurate aerial data in metropolitan areas goes beyond traditional data products because the fast-changing urban environments require more frequent and hence more efficient updates of geospatial base layers.

The Leica CityMapper-2 is specifically designed for airborne urban mapping and offers twice the data collection performance to address this urgent need for 3D data. The world's only hybrid oblique imaging and LiDAR airborne sensors, captures two nadir (RGB/NIR) and four oblique 150 MP images every 0.8 seconds offering highest resolution to visualize every corner of the city. Together with a new generation 2 MHz pulse rate LiDAR, this sensor breaks all conventional barriers of urban mapping.

The newly developed optical system is equipped with Leica Geosystem's unique mechanical forward-motion-compensation (FMC), which allows to capture high quality imagery even in difficult lighting conditions with no reduction in efficiency, unlike traditional camera systems that have to decrease shutter and aircraft speeds to control image blur.

PHOTOMOD 6.5. Productivity and New Functions

D. Kochergin, Racurs, Moscow, Russia

The presentation consists of two main parts. The first one is dedicated to the new features of latest PHOTOMOD system version 6.5: New algorithm for the bundle adjustment, New distributed processing implementation

Radical improvements of the 3D-models building and visualization quality, New 3D-feature extraction tools, the prototype of stereoclient software for OS Android, updated PHOTOMOD Conveyor and more..

Second part tells about the system productivity on recommended hardware configuration for the projects of Racurs production department.

The new PHOTOMOD 6.5:

- New algorithm for the bundle adjustment
 - significant speeding up the adjustment for "pure" block layout (big and instable orientation angle values)
 - full and smart automation of detection of incorrect points
 - multithread calculations support
 - modifications of the self-calibration procedure
- New distributed processing implementation
 - increasing the reliability and resistance to local network failures
 - general speeding up
 - new user interface
 - fast tasks managing, immediate task pausing on remote client machine
 - immediate task starting
 - the capability of viewing LOG-file directly in distributed processing window
 - short report and time statistics
 - possibility of viewing only tasks belonged to selected client
 - equal and consequent workloading of clients
 - export of LOG-files
- Radical improvements of the 3D-models building and visualization quality
 - DSM accuracy and details increasing
 - 3D-model layers and tiles for fast and comfortable displaying
 - json format support
 - high quality texturing
 - DTM – DSM conversion modifications
 - enhancements of satellite imagery 3D-modeling
- New 3D-feature extraction tools
 - more templates for roof digitizing
 - combining, cutting and aligning of 3D vector objects
- "Remote" stereovectorization ("stereoclient")
 - significant speeding up of objects redrawing
- Additional tools for UAS aerial triangulation
- Access to Airbus OneAtlas and DigitalGlobe EarthWatch satellite imagery coverages
- Updated PHOTOMOD Conveyor :
 - OS Linux version
 - REST API interface for cloud services
 - New user interface
 - Automatic coordinate system selection
 - Automatic Ground control points measurements over georeferenced raster object

Automated Generalization

A.S. Kirichenko, A.G. Demidenko, A.E. Kruzhkov, KB Panorama, Moscow, Russia

Nowadays, it is difficult to keep up with the progress: from year to year, new technologies appear, while existing ones get upgraded – all processes are automated, optimized and accelerated.

Information technologies feature a particular growth peak, and electronic cartography does not fall behind. There are many mapping web services in the Internet, and one of their main advantages is the ability to use multi-scale maps containing both overview and detailed cartographic information, which is excellent for analysis and management objectives.

The main difficulty in creating a multi-scale map is the availability of a set of maps of all scales, but even if such set is prepared, their timely updating is also a time-consuming task. The modern world is very dynamic, and regular digitization of all changes and production of new maps requires a huge labor resource. How to automate the process of creating multi-scale maps? The answer is automated generalization.

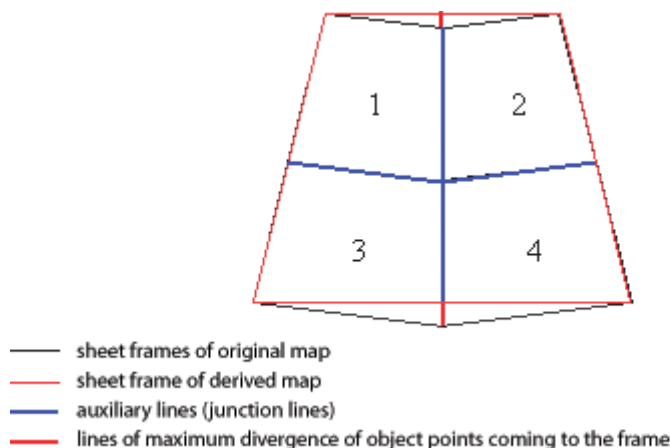
What is the essence of this process? Automated generalization is the automated transformation of a larger-scale map into a smaller-scale map by performing processes such as metric filtering, contour generalization, change of symbols and localization of objects, simplification of hydrography, road networks and settlements.

The generalization process consists of a number of stages:

1. Development of a nomenclature sheet of a derived scale map

When making a generalization, one derived scale map sheet is automatically generated for every four sheets of a digital topographic map of the original scale, for example, 1 sheet of the 1:50,000 scale is generated for 4 sheets of the 1:25,000 scale;

The selection of original scale map sheets is performed automatically by the nomenclature of the derived scale map sheet. In this case, the derived scale map sheet is supplemented with the sheet frame and auxiliary lines. Vertical lines run along the mating vertical sides of sheet frames of the original scale map. Horizontal line - along the mating horizontal sides of sheet frames of the original scale map. Further, objects are crosslinked along the auxiliary lines.

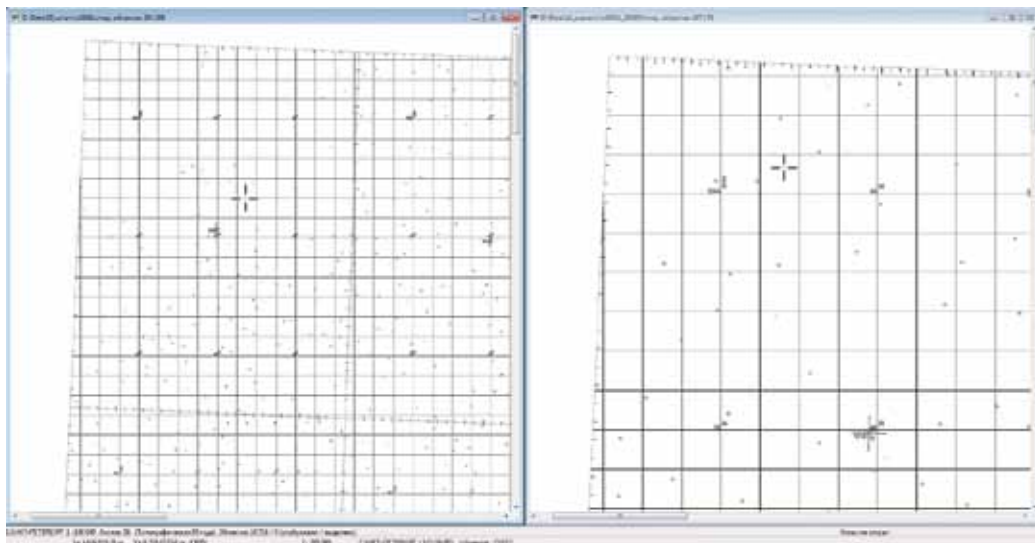


First of all, to avoid divergences when transferring objects from four sheets of the original map to the derived scale map, object points are automatically drawn to the frame of the derived sheet (a thin red line). This automatically simplifies the metric description of linear and areal objects of the map, taking into account existing spatial topological bonds.



The left figure shows objects before the automatic simplification of metric, and the right figure shows objects after this procedure.

At the end of the transfer of objects, objects are stitched along the junction lines, then the mathematical framework is formed. During this process, first mathematical framework objects of the original map are automatically deleted, then mathematical framework objects (horizontal and vertical coordinate lines of the rectangular grid, points of intersection of coordinate lines, parallel and meridian outputs, central cross) are automatically created.



The figure shows updating of mathematical framework objects and rarefaction of field-edit framework objects.

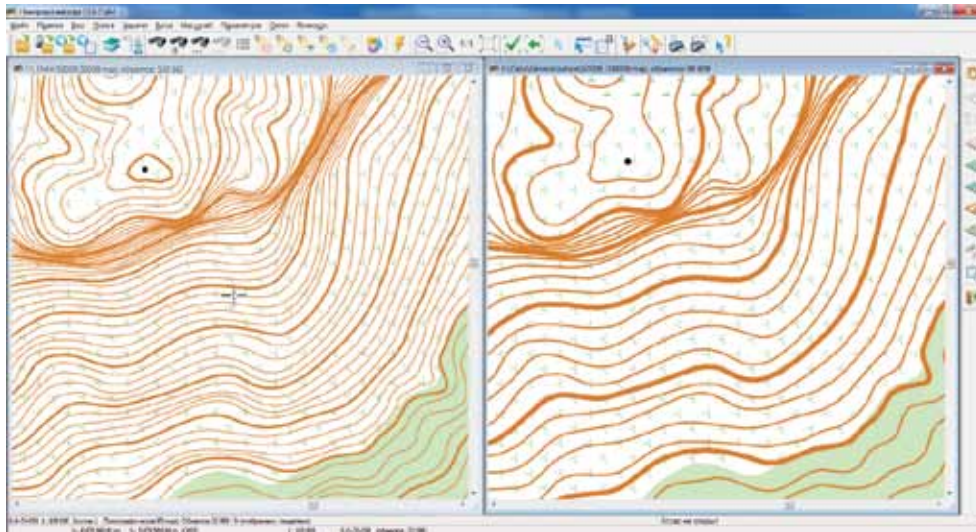
2. Terrain generalization

Terrain generalization includes generalization of contours and point objects of the terrain. During the procedure, contours are either removed or converted to point objects with absolute altitude.

If the contour is not closed, then the multiplicity of its altitude is checked by the given contour interval of the derived map. If the contour altitude is not a multiple of the specified contour interval, the contour is removed.

If the contour is closed and is not a local extremum, it is treated as open. If the closed contour is a local extremum, its area is checked. If the contour area is greater than the threshold value, the contour is not

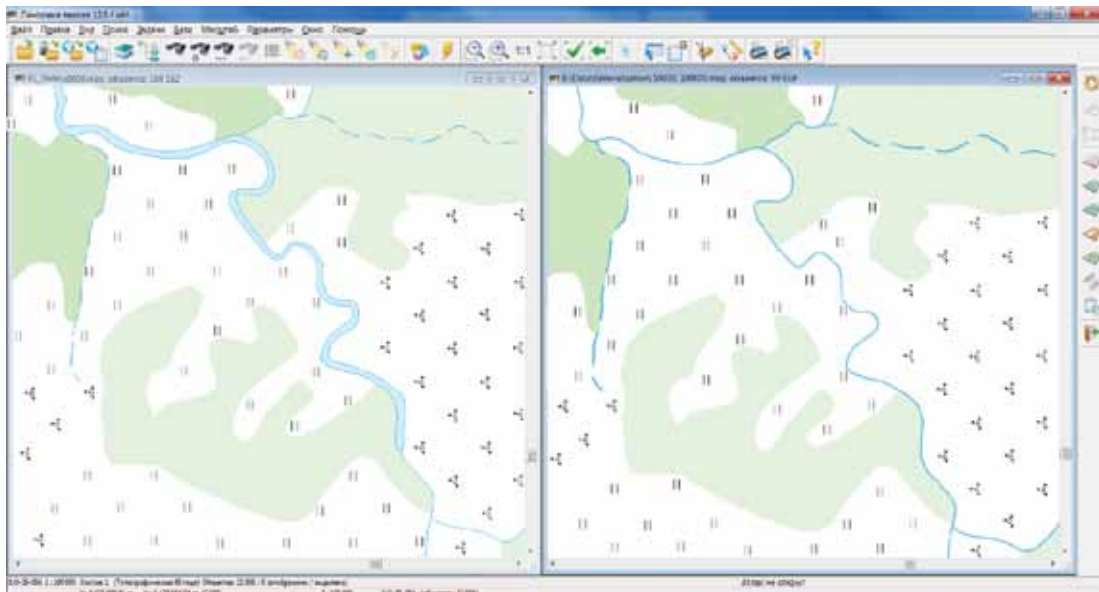
removed. If the contour area is less than the threshold value, it is removed and a point object with absolute altitude is created instead.



The left figure shows contours before generalization, the right - after generalization.

3. Generalization of hydrography and hydraulic structures

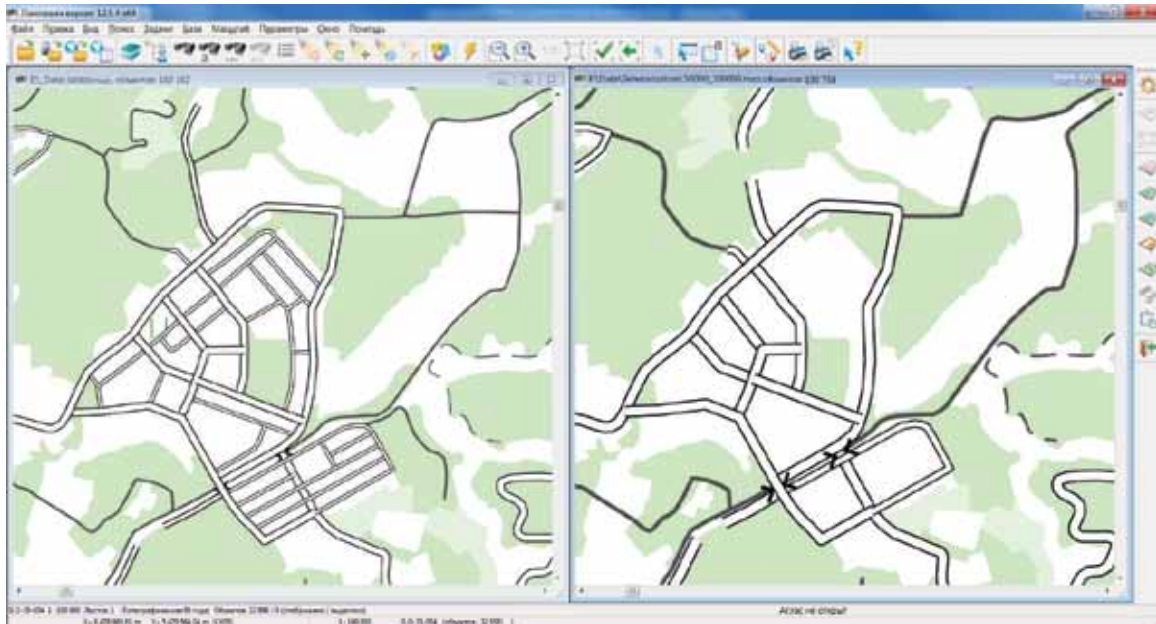
At the 3rd stage of generalization, sections of areal hydrographic objects of a certain width are automatically replaced by sections of linear objects.



The left figure shows the areal river and linear feeders before generalization, the right - after generalization: the river has a linear view, the feeders reach the new metric of the river.

4. Road network generalization

Simplification of linear objects of a road network is made according to the range of visibility assigned to specific objects corresponding to the degree of their significance. The degree of significance of a road is determined by the type, length and nature of its location relative to other roads. Upon the implementation of this objective, less significant roads will not be displayed on a scale smaller than the basic one.



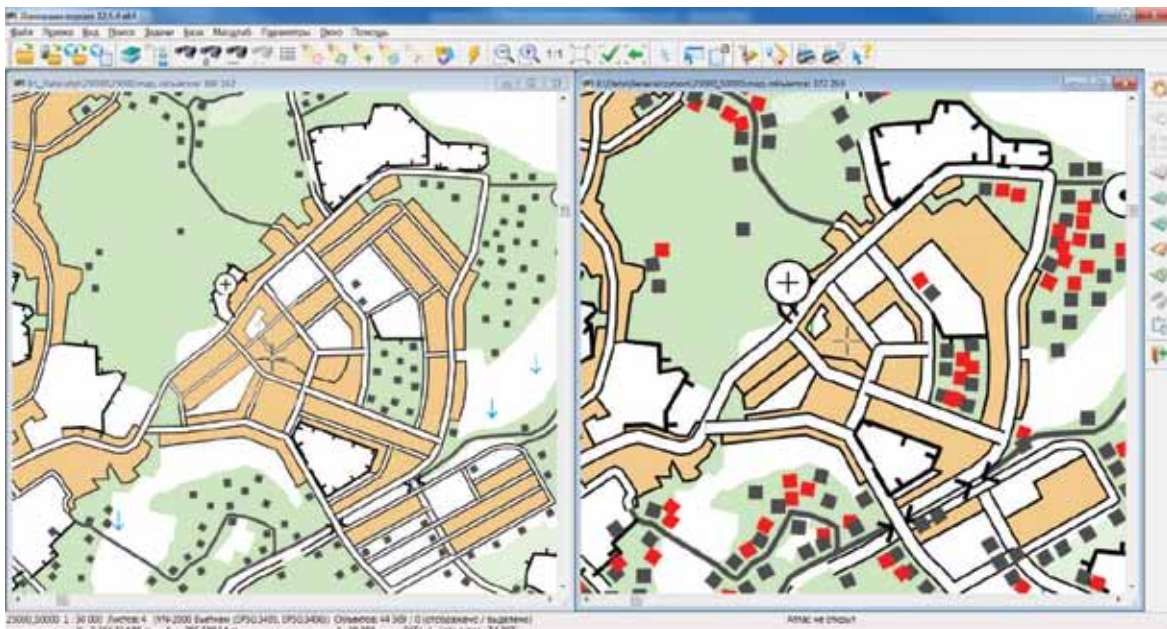
The right figure shows an example of simplification of the road network after generalization

5. Generalization of residential districts in settlements

When processing settlements, the simplification of the road network, cross-linking of residential districts, reduction in the number of buildings of low significance and alignment of buildings relative to nearby roads are performed.

Areal, linear structures and point features of special structures (antenna, hospital, school) have a higher degree of significance. Extra-scale point and vector structures have a small degree of significance.

As a result of settlements' simplification, the map contains selected structures recommended for removal.

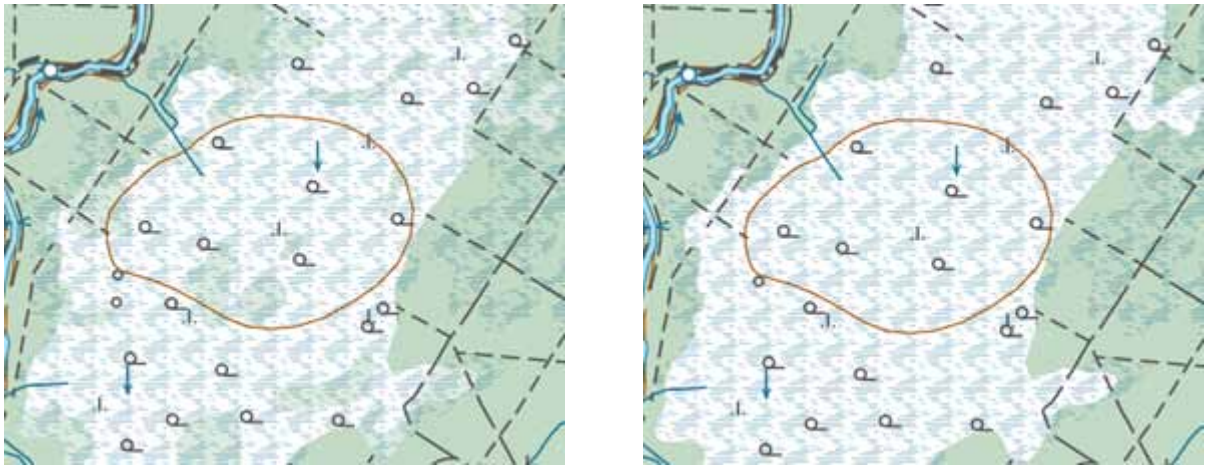


The right figure shows an example of a sampling of buildings of low significance after the alignment relative to nearby roads.

6. Generalization of small-length or small-area objects

At this stage of generalization, nearby linear unclosed objects of short length of the same type and areal objects of the same type are cross linked. Crosslinking of linear objects is performed when placing objects

in the proximity tolerance between the endpoints. Crosslinking of areal objects is performed when placing objects themselves in the proximity tolerance. Objects of small length or area, which are not cross linked, are converted to point objects according to the transcoding table.



The right figure shows the removal of small-area objects — green forests in the swamps — after generalization.

7. Junction with adjacent sheets

The junction of nomenclature sheets of the electronic map implies program-visual control and editing of information about the objects coming to the frame in order to determine unambiguous, consistent characteristics of adjacent objects in accordance with the rules of digital description. If there are junction error messages, the reasons that caused these messages are eliminated, while the procedure is repeated.

After completing the junction of the nomenclature sheets, a visual analysis of processing results is performed.

Conclusion

The main purpose of the automated generalization process is to speed up the process of creating multi-scale maps. For the implementation of this possibility, Design Bureau Panorama has developed a special software "Automated generalization of digital topographic maps", which is an additional module to the professional GIS Panorama. Even now the processing of large areas of maps is accelerated in the software module. On an average performance computer, the conversion of 36 map's sheets of the 1:100,000 scale to 9 map's sheets of the 1:200,000 scale takes less than two hours (up to 15 minutes per sheet).

It should be added that automated generalization is at the stage of its formation, but due to the high demand for this technology, the degree of its automation will increase in the near future.

AIRBORNE SURVEY AND PHOTOGRAMMETRIC MAPPING

The entire territory of the Republic of Crimea in 1:2 000 scale

The entire territory of the Republic of Tatarstan in 1:2 000 scale

11 Russian cities in 1:2 000 scale

1112 Russian towns in 1:10 000 scale

Barabinsk, Ufa, Verkhny Ufaley, Galich, Dankov, Korenovsk, Ruza, Khasavyurt, Volodarsk, Ardon, Tomsk, **VOLGOGRAD,** Dmitrovsk, Skopin, Kalininsk, **Novosibirsk,** Bobrov, Vyatskie Polyany, Nadym, Chebarkul, **PERM,** Lagan, Belaya Kholunitsa, Malgobek, Dudinka, Murashi, Osa, **Omsk,** Tyukalinsk, Pallasovka, Nyandoma, Kamyzyak, **Nizhny Novgorod,** Uzhur, **Yekaterinburg,** Shlisselburg, Khilok, Ak-Dovurak, Mglin, Toropets, Gubakha, Snezhnogorsk, Barysh, Roshal, **Chelyabinsk,** Sursk, Kuritsk, Satka, Sim, Vysotsk, **Rostov-on-Don,** Mozhaysk, Pyt-Yakh, Zherdevka, Langepas, Pikalyovo, Ural, Andreapol, Kasimov, Chukhloma, Zlynka, Ostashkov, Kushva, **KAZAN,** Polyarnie Zory, Venyov, Gdov, Syasstroy, Vytegra, Nazran, **Naberezhnye Chelny,** Tyumen, Emva, Zvenigorod, Kronstadt, Ivdel, Zmeinogorsk, Mozhga, Lyuban, Kulebaki, Relight, Zainsk, Nyazepetrovsk, Lipki, Kozelsk, Yakhroma, Yuryuzan, Bakap, Degtyarsk, Opochka, Aniva, Urzhum, Tarusa, Bapey, Lahdenpohja, Sovetsk, Myshkin, Zadonsk, Volosovo, Kalach, Vorkuta, Kargopol, Svetogorsk, Olenegorsk, Starodub, Khabarovsk, Trubchevsk, Losino-Petrovsky, Asha, Vetluga, Uglegersk, Dukhovschina, Saratov, Makashino, Boguchar, Poshkhonye, Malmyzh, Chkalovsk, Ryazan, Lipetsk, Zakamensk, Toguchin, Srednekolymsk, Kataysk, Severouralsk, Maravitsko, Tomar...



Roscartography

CONNECTING PLACE AND SOLUTIONS

Volgogradsky prospekt, 45, bld 1
Moscow, 109316, Russia

tel.: +7 (499) 177-50-00,

fax: +7 (499) 177-59-00,

e-mail: info@roscartography.ru

www.roscartography.ru

GEOSPATIAL DATA FOR THE ENTIRE TERRITORY OF RUSSIAN FEDERATION

Scientific Committee



Media partners



GISCAFÉ



Contacts

Racurs Co.
13A, Yaroslavskaya Str., Moscow, 129366, Russia
Tel: +7 495 720 51 27 | conference@racurs.ru
<http://conf.racurs.ru>

